Primljen / Received: 3.2.2015.
Ispravljen / Corrected: 19.4.2015.
Prihvaćen / Accepted: 2.5.2015.
Dostupno online / Available online: 10.5.2016.

Study of ballast layer stiffness in railway tracks

Authors:

Assoc.Prof. Jabbar Ali Zakeri, PhD. CE
The Center of Excellence in Railway Transportation
Iran University of Science and Technology
Teheran, Iran
zakeri@iust.ac.ir

Seyed Ali Mosayebi, MSc. CE
Iran University of Science and Technology
Teheran, Iran
mosayebi@iust.ac.ir

Professional paper

Jabbar Ali Zakeri, Seyed Ali Mosayebi

Study of ballast layer stiffness in railway tracks

In this paper, ballast layer stiffness in railway tracks is investigated. Test results show that the percentage of ballast contamination changes considerably across the ballast layer depth. For this reason, the ballast was divided during modelling into three layers and the stiffness of each layer was derived based on the pyramid model developed for that purpose. The results show that the stiffness exhibited by the bottom ballast layer exceeds by up to 20 % that of the top and middle layers.

Key words:
field and laboratory tests, contamination, fine particles, ballast layer stiffness, pyramid model

Stručni rad

Jabbar Ali Zakeri, Seyed Ali Mosayebi

Ispitivanje krutosti zastorne prizme željezničkog kolosijeka

U radu je analiziran utjecaj onečišćenja zastorne prizme na njezinu krutost. Rezultati ispitivanja pokazali su da se postotak onečišćenja zastora značajno mijenja s obzirom na debljinu zastorne prizme. Zbog toga je zastor tijekom isptivanja podijeljen u tri sloja, a krutost svakog sloja određena je primjenom modela piramide koji je određen za taj slučaj. Rezultati su pokazali da donji sloj zastorne prizme ima veću krutost u odnosu na površinski i srednji sloj i do 20 %.

Ključne riječi:
terensko i laboratorijsko ispitivanje, onečišćenje, sitne čestice, krutost zastorne prizme, model piramide

Fachbericht

Jabbar Ali Zakeri, Seyed Ali Mosayebi

Untersuchungen zur Steifigkeit des Bettungskörpers bei Eisenbahngleisen

In dieser Arbeit wird der Einfluss von Verunreinigungen des Bettungskörpers auf seine Steifigkeit durchgeführt. Die Resultate der Untersuchungen zeigen, dass der Anteil verunreinigten Schotters stark in Abhängigkeit von der Stärke des Schotterbetts variiert. Daher wurde das Schotterbett bei der Modellierung in drei Abschnitte unterteilt, so dass für jeden Teil die Steifigkeit für den entsprechenden Fall mittels des Pyramidenmodells ermittelt werden konnte. Den Resultaten folgend, weist die untere Schicht des Bettungskörpers im Gegensatz zu der mittleren und der oberen Schicht eine bis zu 20 % grössere Steifigkeit auf.

Schlüsselwörter:
Feld- und Laborversuche, Verunreinigung, kleine Partikel, Schottersteifigkeit, Pyramidenmodell

1. Introduction

The railway ballast layer, as a significant part of the railway track system, must fulfil the following important objectives: transfer the stress, create a high resistance to longitudinal and lateral displacement of sleepers, increase elasticity property, increase the longitudinal and lateral stability of railway tracks, and enable easy repair and maintenance of railway tracks. To achieve the mentioned objectives, the railway ballast should be resistant and hard, resistant to weather conditions, resistant to water absorption, resistant to crushing by passing trains, characterized by suitable gradation, sufficiently elastic, and should have other favourable properties. Therefore, laboratory experiments for controlling the quality of materials are necessary. Several studies have been made in this field including those proposed by Indraratna and Salim [1], Selig and Waters [2], and Lim [3]. Some factors are known to be responsible for the decrease of ballast efficiency in railway tracks. One of major factors of this kind is the contamination of ballast. This phenomenon causes deterioration of elasticity properties, decrease of ballast drainage capabilities, and increase in noise and vibration. The influence of coal dust on railway ballast was studied by Tutumluer and Dombrow [4]. In desert areas, the wind-borne sand penetrates in the railway ballast layer, contaminating the ballast and reducing performance of ballasted railway tracks. Zakeri [5] investigated maintenance of railway tracks in a desert area. In these areas, track elasticity properties are known to deteriorate quite considerably. In this respect, Zakeri et al. [6, 7] studied the effects of fouling ballast on the train induced vibrations. One of important parameters in railway tracks is stiffness, which is effective in dynamic analysis of railway tracks. Puzavac et al. [8] investigated the effects of track stiffness on the railway track behaviour. Zhai et al. [9] presented the cone model, which is used for studying the train – track interaction. Also, the train – track interaction models were also used in the following studies: Zakeri and Xia [10], Ripke and Knothe [11], Oscarsson [12], and Oscarsson and Dahlberg [13]. The field and laboratory gradation tests across the ballast layer depth, and derivation of ballast layer stiffness, have not been considered in these studies. In this paper, the investigations started with the study of gradation and distribution of aggregates across the depth of the ballast layer, based on the field and laboratory test results. Then the ballast layer was divided into three layers, and the stiffness of each layer was derived using the pyramid model.

2. Modelling of ballast layer in railway track analysis

Traditional railway track superstructure, including the rail, sleeper and fastening system, is supported by the ballast layer. Ballast materials have a uniform gradation and they typically include aggregates ranging from 30 to 60 mm in size. The main task of the ballast layer is to:

a) transfer vertical, horizontal and lateral forces to lower layers
b) maintain the railway track in fixed position
c) provide for elasticity of track and absorption of energy
d) ensure drainage of surface water
e) set and level the surface of the rail track
f) attenuate the shocks, vibrations and noise due to moving railway vehicles
g) act as an insulator for underlying layers
h) prevent growth of plants in railway track.

Factors that have adverse effects on ballast layer properties are:

a) vehicle service load
b) wear in tamping operation
c) ballast fouling due to fall of materials on the track
d) growth of plants or atmospheric and environmental factors like frost
e) change in temperature, and other factors [1, 2].

Minimum thickness of ballast under the sleepers is 30 cm, and the distance between sleepers is 60 cm. For high speed railways, a minimum ballast layer thickness of 40 cm is recommended. However, the ballast layer thickness of at least 45 cm is suggested to provide for proper resistance to lateral displacements. Standard specifications of railway track parts are presented in Leaflet No. 301 [14]. The ballast sample gradation based on this Leaflet is shown in Figure 1.

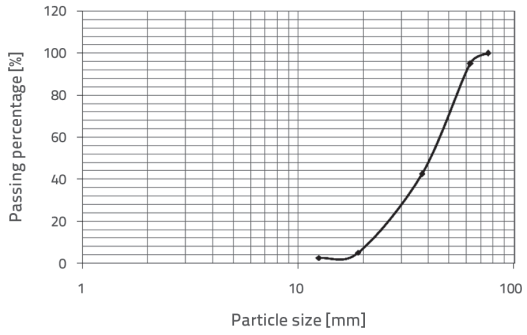

Figure 1. Ballast sample grading based on Leaflet No. 301

Many models are currently used for the dynamic analysis of railway structures. Numerical models of railway tracks, based on the consideration of masses under the rail, can be grouped in the following three categories:

a) lumped masses
b) beam on continuous foundation
c) beam on elastic discrete supports.

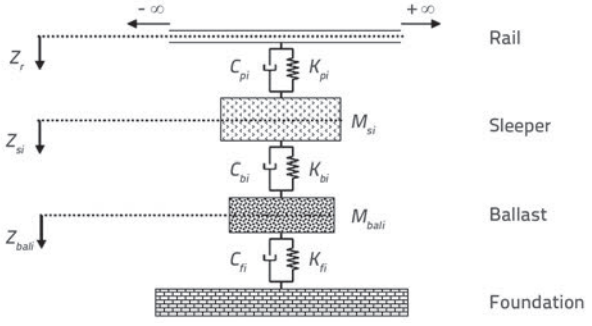

Figure 2. Ballasted track with three layers

In order to evaluate the effect of ballast on the railway track analysis, the ballast layer is considered as a mass spring model under the sleepers. Also, the ballast layer can be modelled as 1, 2 and 3 layers, each of which is modelled as a lumped mass in the dynamic analysis of railway structures. Figure 2 shows a ballasted railway track with three layers including rail, sleeper and ballast, .

Since the distribution of the contamination material and fine aggregates changes across the depth of the ballast layer, the model of ballast with three layers is more accurate for the railway dynamic analysis, when compared to the single layer model. For this reason, the distribution of ballast aggregates across the ballast layer depth is investigated in the next section through field and laboratory tests.

3. Analysis of ballast aggregate distribution through field and laboratory investigations

The percentage of the contamination material and fine aggregates in ballast layer increases with the passage of trains. Sources of ballast contamination in railway track can be divided into the following five categories:

a) failure of ballast aggregates due to thermal stress, freezing, climatic factors, and railway traffic
b) penetration of particles, such as atmospheric dust, into the ballast layer
c) wear of sleepers
d) penetration of particles from lower layers into the ballast layer
e) penetration through the superstructure.

Some methods for assessing contamination in ballast layers are: isotope method, measuring machine, visual inspection and sampling tests [1, 2].

A ballasted railway track in Iran was selected for the evaluation of aggregate distribution across the depth of ballast layers through field and laboratory tests (Figure 3). Specifications for the track under study are: rail: UIC 60, concrete sleepers: B70, fastening systems: Vossloh SKL 14, age of track: 25 years, tonnage: 5 million tons per year, climate: moderate, maximum train speed: 120 km/h, axle load: 200 kN, usage: freight – passenger railway track. Ballast sampling was accomplished at five specified points named A, B, C, D and F, positioned at suitable distances from each other. After sampling, the ballast samples were studied in laboratory.

Figure 3. Ballasted railway track

After various investigations regarding the testing and sampling tool, a cylindrical sheet 2 mm in thickness, 60 cm in height, and 27 cm in diameter, was finally adopted. These dimensions were selected as they prevent distortion and deformation of the sheet, and corrosion and crushing of ballast materials. The cylinder was divided into three equal parts each 15 cm in height. The three parts were separated with galvanized metal drawers. These parts were separated until samples from three ballast layers were provided for gradation tests. Figures 4 and 5 show the cylindrical metal sheet, and the sampling from the top, middle and bottom ballast layers.

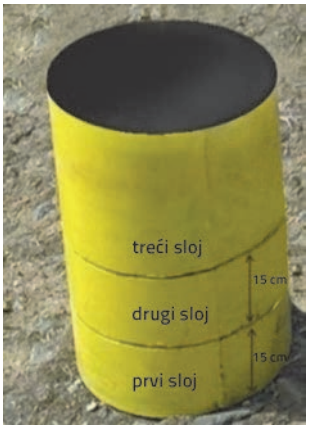

Figure 4. Cylindrical metal sheet

Figure 5. Sampling from ballast layers: a) sampling from top layer; b) sampling from middle layer; c) sampling from bottom layer

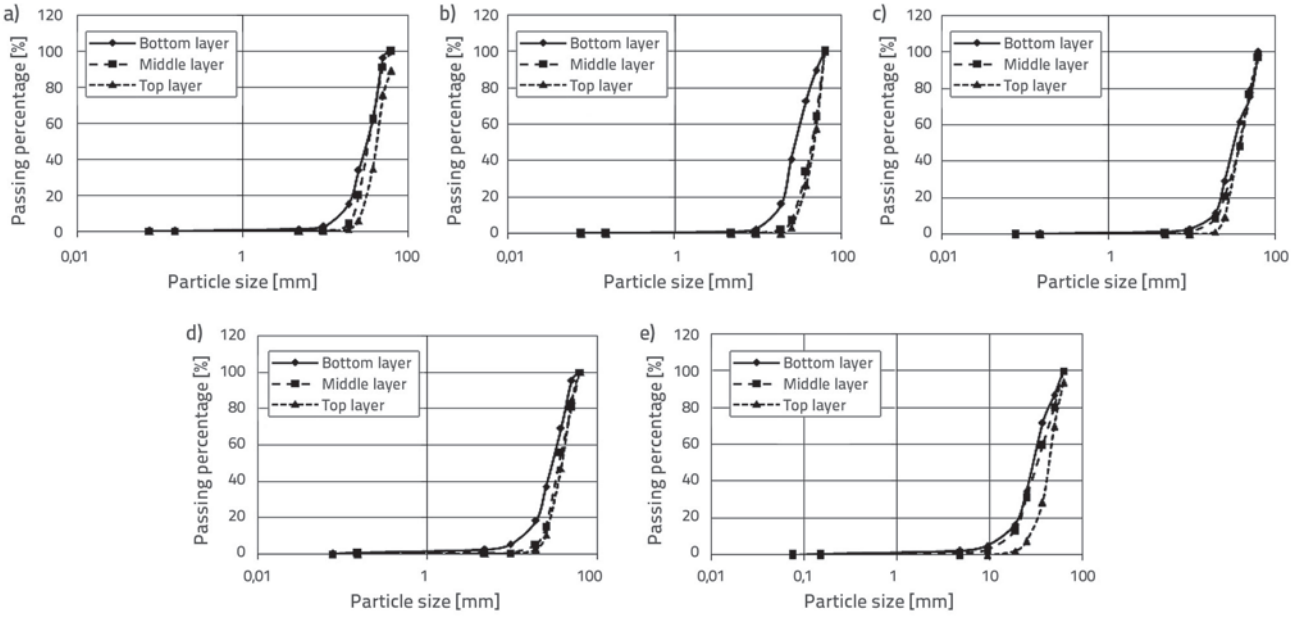

Figure 6. Passing percentage for various points based on field and laboratory tests: a) Point A; b) Point B; c) Point C; d) Point D; e) Point F

After sampling, the samples were tested in laboratory where they were first dried in oven. Then aggregates were passed through various sieves. After shaking the sieves and screening the railway ballast materials, the remaining and passing percentages for ballast layers were measured. Gradation results for ballast layers, including the bottom, middle and top layers for five points, are presented in Figure 6.

As can be observed, the bottom layer has a greater passing percentage when compared to the middle and top layers. Also, the middle layer has a greater passing percentage than the top layer. For examining the contamination percentage in the depth of ballast layers, the passing percentage from the sieve No. 3/4, 19 mm in diameter was considered. The contamination content, based on percentage for each ballast layer in each point, is presented in Figure 7.

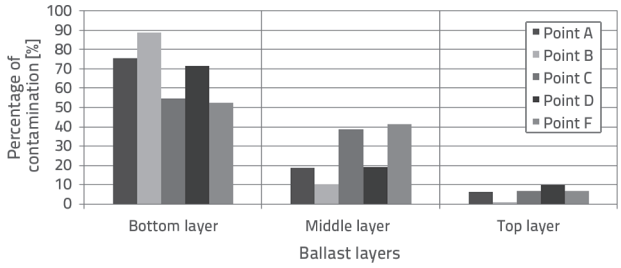

Figure 7. Percentage of contamination for each ballast layer at various points

As can be seen in Figure 7, the contamination percentage for the bottom layer is greater at all points than that registered in the middle and top layers. Also, an average contamination percentage for the bottom, middle and top ballast layers amounts to 68, 26, and 6 percent, respectively. The passing percentage values for the 4.75 mm sieve No. 4 were considered to evaluate the fine aggregate content across the depth of ballast layers. The fine aggregate content based on the percentage for each ballast layer at each point is presented in Figure 8.

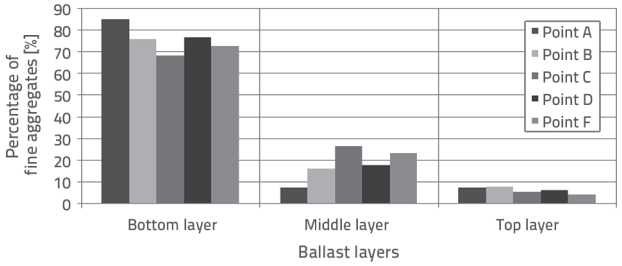

Figure 8. Percentage of fine aggregates for each ballast layer at various points

As can be seen, the percentage of fine aggregates is greater at all points in the bottom layer compared to the middle and top layers. Also, an average percentage of fine aggregates for the bottom, middle and top ballast layers amounts to 76 %, 18 %, and 6 %, respectively. Because the contamination and fine aggregate content change significantly across the depth of ballast layers, the ballast model with three layers is more accurate for investigating the effects of ballast in the analysis of railway tracks. For this reason, the stiffness of each ballast layer is derived in the next section using the developed pyramid models.

4. Derivation of ballast layer stiffness by using pyramid model

In the dynamic railway-track analysis, the ballast layer is modelled as a series of springs and dampers placed under the sleepers. Transmission of load from a sleeper to ballast is

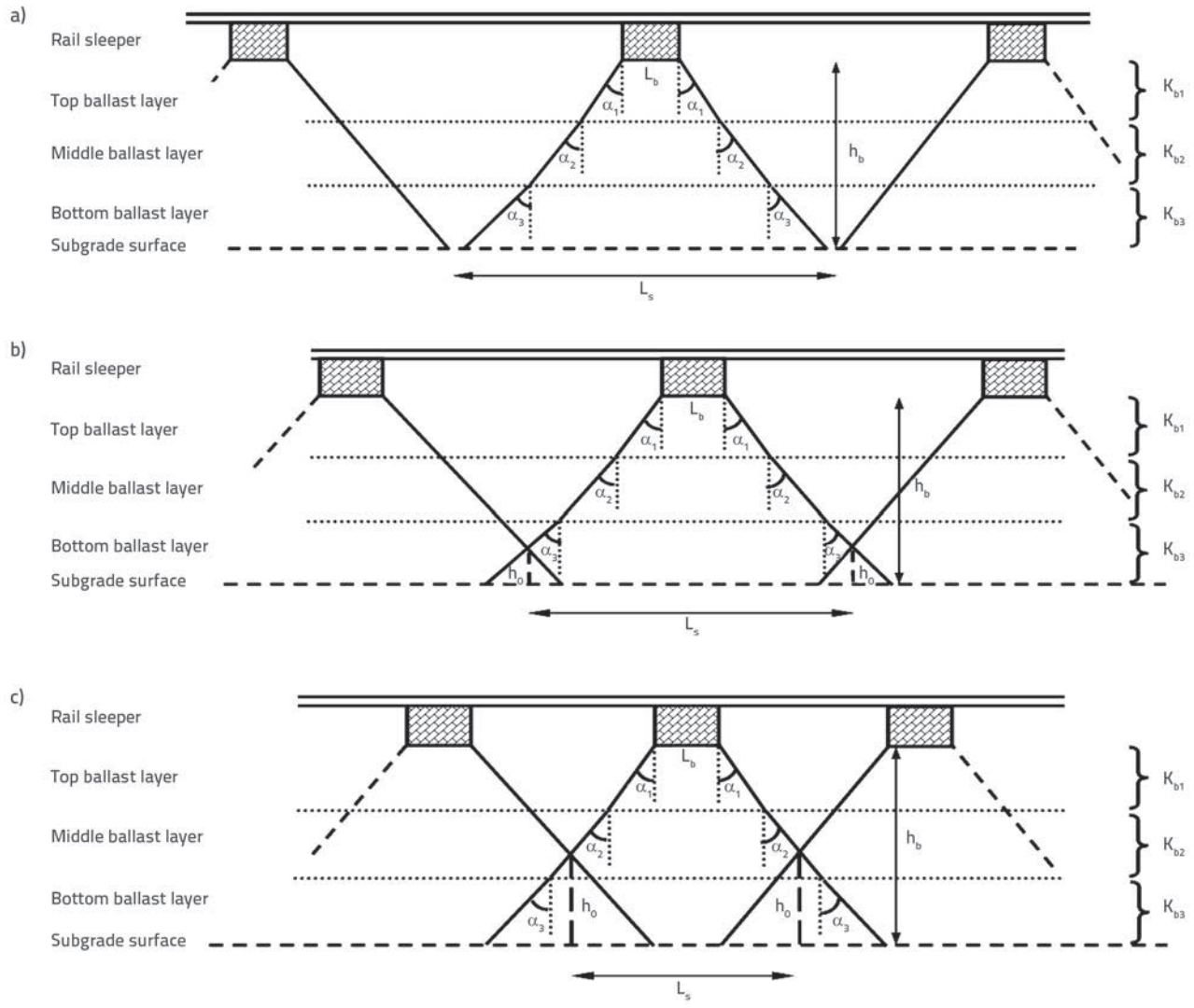

Figure 9 Ballast with three layers: a) ballast without overlap; b) ballast with overlap in the bottom layer; c) ballast with overlap in the middle layer

approximately coincident with conical distribution. This means that ballast stresses are uniformly distributed around the cone area, and that these stresses amount to zero outside the cone. The cone slope is the angle of stress distribution in the ballast layer. Therefore, the stiffness of a ballast layer under the sleepers can be measured using the pyramid model [9]. According to explanations presented in previous sections, the fine aggregate content and contamination of ballast increased in the depth of the ballast layer based on field and laboratory tests. For this reason, the ballast layer can be modelled precisely in the railway track analysis. Consequently, ballast can be divided into three layers and then the stiffness of each layer can be derived based on the developed pyramid model. The ballast with three layers is shown in Figure 9. As can be seen in this Figure, there are three ballast overlapping scenarios:

a) ballast without overlap
b) ballast with overlap in the bottom layer
c) ballast with overlap in the middle layer.

In Figure 9, L_s, L_b and h_b are the distance between sleepers, sleeper width, and ballast layer depth, respectively. Also, α_1, α_2, and α_3 are stress distribution angles at the top, middle and bottom ballast layers. When locating the train wheels between railway sleepers, pyramid forms occur in both adjacent supports. Also, the distribution angle of stress increases by increasing the ballast layer depth or fine aggregate content. Therefore, the probability of overlapping between adjacent ballast layers increases, especially in lower ballast layers. The ballast layer distribution angles could range from 25 to 37 degrees with an increase in the ballast layer depth [15]. The location and extent of ballast overlap with adjacent ballast layers should be examined before calculating the stiffness of ballast layers based on the developed pyramid model. Generally, there are three areas for the top, middle and bottom ballast layers. The important point is that the stiffness of each layer that overlaps with adjacent ballast layers is calculated as a series combined of sections with and without overlap in the same layer. According

Table 1. Stiffness derived for each ballast layer without overlap

Ballast layers	Derived stiffness
Top	$K_1 = \frac{2(l_e - l_b)tg\alpha_1}{\ln\left[\left(\frac{l_e}{l_b}\right)\left(\frac{l_b + 2h_1tg\alpha_1}{l_e + 2h_1tg\alpha_1}\right)\right]}E_1$
Middle	$K_2 = \frac{2(l_e - l_b)tg\alpha_2}{\ln\left[\left(\frac{l_e + 2h_1tg\alpha_1}{l_b + 2h_1tg\alpha_1}\right)\left(\frac{l_b + 2h_1tg\alpha_1 + 2h_2tg\alpha_2}{l_e + 2h_1tg\alpha_1 + 2h_2tg\alpha_2}\right)\right]}E_2$
Bottom	$K_3 = \frac{2(l_e - l_b)tg\alpha_3}{\ln\left[\left(\frac{l_e + 2h_1tg\alpha_1 + 2h_2tg\alpha_2}{l_b + 2h_1tg\alpha_1 + 2h_2tg\alpha_2}\right)\left(\frac{l_b + 2h_1tg\alpha_1 + 2h_2tg\alpha_2 + 2h_3tg\alpha_3}{l_e + 2h_1tg\alpha_1 + 2h_2tg\alpha_2 + 2h_3tg\alpha_3}\right)\right]}E_3$

Table 2. Stiffness derived for each ballast layer with overlap at the bottom layer

Ballast layers		Derived stiffness
Top		$K_1 = \frac{2(l_e - l_b)tg\alpha_1}{\ln\left[\left(\frac{l_e}{l_b}\right)\left(\frac{l_b + 2h_1tg\alpha_1}{l_e + 2h_1tg\alpha_1}\right)\right]}E_1$
Middle		$K_2 = \frac{2(l_e - l_b)tg\alpha_2}{\ln\left[\left(\frac{l_e + 2h_1tg\alpha_1}{l_b + 2h_1tg\alpha_1}\right)\left(\frac{l_b + 2h_1tg\alpha_1 + 2h_2tg\alpha_2}{l_e + 2h_1tg\alpha_1 + 2h_2tg\alpha_2}\right)\right]}E_2$
Bottom	Without overlap	$K_{31} = \frac{2(l_e - l_b)tg\alpha_3}{\ln\left[\left(\frac{l_e + 2h_1tg\alpha_1 + 2h_2tg\alpha_2}{l_b + 2h_1tg\alpha_1 + 2h_2tg\alpha_2}\right)\left(\frac{l_b + 2h_1tg\alpha_1 + 2h_2tg\alpha_2 + 2h_{31}tg\alpha_3}{l_e + 2h_1tg\alpha_1 + 2h_2tg\alpha_2 + 2h_{31}tg\alpha_3}\right)\right]}E_3$
	With overlap	$K_{32} = \frac{2l_stg\alpha_3}{\ln\left[\left(1 + \frac{2h_{32}tg\alpha_3}{l_e + 2h_1tg\alpha_1 + 2h_2tg\alpha_2 + 2h_{31}tg\alpha_3}\right)\right]}E_3$

Table 3. Stiffness derived for each ballast layer with overlap at the middle layer

Ballast layers		Derived stiffness
Top		$K_1 = \frac{2(l_e - l_b)tg\alpha_1}{\ln\left[\left(\frac{l_e}{l_b}\right)\left(\frac{l_b + 2h_1tg\alpha_1}{l_e + 2h_1tg\alpha_1}\right)\right]}E_1$
Middle	Without overlap	$K_{21} = \frac{2(l_e - l_b)tg\alpha_2}{\ln\left[\left(\frac{l_e + 2h_1tg\alpha_1}{l_b + 2h_1tg\alpha_1}\right)\left(\frac{l_b + 2h_1tg\alpha_1 + 2h_{21}tg\alpha_2}{l_e + 2h_1tg\alpha_1 + 2h_{21}tg\alpha_2}\right)\right]}E_2$
	With overlap	$K_{22} = \frac{2l_stg\alpha_2}{\ln\left[\left(1 + \frac{2h_{22}tg\alpha_2}{l_e + 2h_1tg\alpha_1 + 2h_{21}tg\alpha_2}\right)\right]}E_2$
Bottom		$K_3 = \frac{2l_stg\alpha_3}{\ln\left[\left(1 + \frac{2h_3tg\alpha_3}{l_e + 2h_1tg\alpha_1 + 2h_{21}tg\alpha_2 + 2h_{22}tg\alpha_2}\right)\right]}E_3$

Table 4. Stiffness ratio for ballast layer 30 cm in depth

Cases	1			2			3			4		
Ballast layers	top	middle	bottom	top	middle	bottom	top	middle	bottom	top	middle	bottom
Distribution angle of stress [°]	25	31	37	28	34	40	31	37	43	34	40	46
Overlap layer	bottom layer			bottom layer			bottom layer			bottom layer		
Overlap value [cm]	2.5			5			7			9		
K_2/K_1	1.25			1.3			1.35			1.41		
K_3/K_1	1.5			1.57			1.62			1.65		

Table 5. Stiffness ratio for ballast layer 45 cm in depth

Cases	1			2			3			4		
Ballast layers	top	middle	bottom	top	middle	bottom	top	middle	bottom	top	middle	bottom
Distribution angle of stress [°]	25	31	37	28	34	40	31	37	43	34	40	46
Overlap layer	bottom layer			middle layer			middle layer			middle layer		
Overlap value [cm]	14.5			17.6			20.3			22.6		
K_2/K_1	1.44			1.5			1.56			1.6		
K_3/K_1	1.67			1.68			1.7			1.7		

to the presented explanations, the stiffness of the top, middle and bottom ballast layers was derived by the authors based on the pyramid model developed for three cases: without overlap, overlap at the bottom, and overlap at the middle ballast layer. Tables 1, 2 and 3 present stiffness results derived by the authors based on pyramid model for each ballast layer without overlap, with overlap at the bottom layer, and with overlap at the middle layer, respectively.

In these Tables, L_e and L_b are the effective support length of half sleeper, and the sleeper width, respectively. Also, h_1, h_2 and h_3 are the thickness of the top, middle and bottom ballast layers, respectively. E_1, E_2 and E_3 are the elastic moduli for the top, middle and bottom ballast layers, respectively. The stiffness ratio of ballast layers for ballast 30 cm in depth, and for various distribution angles, is shown in Table 4. The location and extent of overlap are also presented in this Table.

As can be seen in Table 4 for ballast 30 cm in depth, the overlap value increased in case of an increase in the distribution angle. Also, the overlap occurred in the bottom ballast layer for all types. The stiffness ratio of the middle layer to top layer, and the stiffness ratio of the bottom layer to top layer, increase in case of an increase in the distribution angle of stress.

The stiffness ratio of ballast layers, and the ballast overlap location and extent, are shown in Table 5 for various distribution angles and for the ballast layer 45 cm in depth.

As shown in Table 5 for ballast 45 cm in depth, the overlap value increases with an increase in the distribution angle. Also, the location of overlap moved to the middle layer with an increase in the distribution angle. The stiffness ratio of the middle layer to top layer, and the stiffness ratio of the bottom layer to top layer increase with an increase in the distribution angle of stress.

5. Conclusion

Considering that the railway ballast is one of important parts of railway tracks, it is clear that this segment of the railway system should be closely examined and controlled. Since the presence of contamination and fine aggregates in the ballast layer can affect its efficiency, the investigation of ballast gradation is essential, and must be conducted in the scope of field and laboratory tests. In this research, gradation tests were conducted on railway ballast samples for five points at the ballasted railway track in Iran, and percentages of fine aggregates and contamination were calculated for each ballast layer. The ballast layer was then divided into three layers and the stiffness of each ballast layer was derived based on the developed pyramid model. The important findings obtained can be summarized as follows:

1. The percentage of contamination and fine aggregates is greater at the bottom ballast layer compared to the middle and top ballast layers.
2. An average contamination percentage for the bottom, middle and top ballast layers amounts to 68 %, 26 %, and 6 %, respectively.

3. An average fine aggregate percentage for the bottom, middle and top ballast layers amounts to 76 %, 18 %, and 6 %, respectively.
4. Based on the developed pyramid model, it can be concluded that the stiffness of the bottom ballast layer is greater than that of the middle and top ballast layers. Also, an average stiffness ratio of the bottom to top ballast layer is greater by 20 and 11 percent with respect to the stiffness ratio of the middle to top ballast layer, for the ballast depth of 30 and 45 cm, respectively.
5. By increasing the angle of stress distribution in the ballast layer from low to high values, the stiffness values of ballast layers increase for all ballast depths. Also, the stiffness ratio of the middle to top ballast layer for the ballast depth of 45 cm is greater by 15.2, 15.4, 15.5 and 13.5 percent with respect to ballast depth of 30 cm.
6. The ballast overlap values increase when the angle of stress distribution in the ballast layer is increased from low to high values. Also, the stiffness ratio of the bottom to top ballast layer for the ballast depth of 45 cm is greater by 11.3, 7, 5 and 3 percent with respect to the ballast depth of 30 cm.
7. The ballast model with three layers is more accurate for studying the effects of ballast layer on the railway track analysis because of significant variations in the level of contamination, fine aggregate content, and stiffness, across the depth of the ballast layer.

REFERENCES

[1] Indraratna, B., Salim, W.: *Mechanics of Ballasted Rail Tracks, A Geotechnical Perspective*, London: Taylor & Francis/Balkema, 2005.

[2] Selig, E.T., Waters, J.M.: *Track Geotechnology and Substructure Management*, London: Thomas Telford, 1994.

[3] Lim, W.L.: *Mechanics of railway ballast behavior*, University of Nottingham, degree of Doctor of Philsophy, 2004.

[4] Tutumluer, E., Dombrow, W., Huang, H.: Effect of coal dust on railroad ballast strength and stability, *8th International Conference on Bearing Capacity of Roads, Railways and Airfields*, The University of Illinois at Urbana-Champaign, Illinois, USA, 2009.

[5] Zakeri, J. A.: Investigation on Railway Track Maintenance in sandy-dry Areas, *Journal of structure and infrastructure engineering*, 8 (2012) 2, pp. 135-140, http://dx.doi.org/10.1080/15732470903384921

[6] Zakeri, J.A., Abbasi, R.: Field investigation on distribution of contact pressure between sleeper and saturated ballast with flowing sand, *11th International conference on Railway Engineering*, London, Uk, 2011.

[7] Zakeri, J.A., Esmaeili, M., Mosayebi, S.A., Abbasi, R.: Effects of vibration in desert area caused by moving trains, *Journal of Modern Transportation*, 20 (2012) 1, pp. 16-23, http://dx.doi.org/10.1007/BF03325772

[8] Puzavac, L., Popovic, Z., Lazarevic, L.: Influence of Track Stiffness on Track behavior under Vertical Load, *Traffic&Transportation*, 24 (2012) 5, pp. 405-412, http://dx.doi.org/10.7307/ptt.v24i5.1176

[9] Zhai, W.M., Wang, K.Y., Lin, J.H.: Modelling and Experiment of Railway Ballast Vibrations, *Journal of Sound and Vibration*, 270 (2004) 4-5, pp. 673–683, http://dx.doi.org/10.1016/S0022-460X(03)00186-X.

[10] Zakeri, J.A., Xia, H.: Sensitivity Analysis of Track Parameters on Train-Track Dynamic Interaction, *Journal of Mechanical Science and Technology*, 22 (2008) 7, pp. 1299-1304, http://dx.doi.org/10.1007/s12206-008-0316-x

[11] Ripke, B., Knothe, K.: Simulation of High Frequency Vehicle-Track Interactions, *Vehicle System Dynamics*, Supplement, 24 (1995), pp. 72-85, http://dx.doi.org/10.1080/00423119508969616

[12] Oscarsson, J.: *Dynamic Train / Track / Ballast Interaction – linear and State – Dependent Track Models*, Licentiate Thesis, Chalmers University of Technology, Goteborg, 1999.

[13] Oscarsson, J., Dahlberg, T.: Dynamic Train / Track / Ballast Interaction – Computer Models and Full-Scale Experiments, *Vehicle System Dynamics*, Supplement 28 (1998), pp. 73-84, http://dx.doi.org/10.1080/00423119808969553

[14] Technical and general specification of Ballasted Railway, Leaflet No 301, Management and planning organization of Iran, 2002.

[15] Ahlbeck, D.R., Meacham, H.C., Prause, R.H.: The development of analytical models for railroad track dynamics, *Railroad Track Mechanics & Technology (ed.* Kerr, A.D.), Pergamon Press, Oxford, 1978.